*Desalination and Water Treatment*
www.deswater.com

doi: 10.1080/19443994.2013.770195

51 (2013) 5608–5616
August

Taylor & Francis
Taylor & Francis Group

# Effect of heat treatment on copper removal onto manure-compost-activated carbons

Muhammad Abbas Ahmad Zaini[a,*], Mohd. Azizi Che Yunus[a], Siti Hamidah Mohd. Setapar[a], Yoshimasa Amano[b,c], Motoi Machida[b,c]

[a]*Centre of Lipids Engineering and Applied Research, Universiti Teknologi Malaysia, 81310 Skudai, Johor, Malaysia*
*Tel. +6 07 5535552; Fax: +6 07 5588166; email: abbas@cheme.utm.my*
[b]*Safety and Health Organization, Chiba University, Yayoi-cho 1-33, Inage-ku, Chiba 263-8522, Japan*
[c]*Graduate School of Engineering, Chiba University, Yayoi-cho 1-33, Inage-ku, Chiba 263-8522, Japan*

Received 31 May 2012; Accepted 23 December 2012

---

**ABSTRACT**

The work was aimed to investigate the effect of heat treatment of manure-compost-based activated carbons on the adsorption of copper from aqueous solution. Activated carbons were characterized according to physical structures and surface functional groups. All equilibrium data of activated carbons formerly treated at different temperatures obeyed Langmuir model to linear approximation. Results showed that copper ions favorably adsorbed onto the mesopores at lower equilibrium concentrations and subsequently changed to the micropores at higher equilibrium concentrations. It was found that the increase in electron density upon heat treatment offered higher tendency for the uniform amount of protons to occupy the surface sites. Analysis of Scatchard plots suggested that the affinity driven by the mesopores toward copper ions was stronger than that of the micropores.

*Keywords:* Activated carbon; Cattle-manure-compost; Copper; Heat treatment; Isotherm; Scatchard plot

---

## 1. Introduction

Copper-contaminated wastewater has become one of the most serious environmental problems nowadays. Elevated level of copper ions present in water originates from a variety of industries and sources such as industrial discharge, weathering of soil, fertilizer, paints, and sewage treatment plants [1,2]. The removal of copper ions has become a subject of special concern due to its recalcitrance and persistence in the environment. Copper ions are toxic, not biodegradable and easily accrue in human body, thereafter can cause a number acute and chronic health effects. Reported copper poisoning includes gastrointestinal disturbances, Wilson disease, Menkes syndrome, methaemoglobinemia and renal failure [1,3]. According to World Health Organization, the permissible concentration of copper in drinking water is limited to 2 mg/L [3].

The apparent impact of copper to the environment has triggered for strong preventive measures. Conventional methods for removing copper from water include electrochemical treatment, reverse osmosis,

---

*Corresponding author.

precipitation and coagulation, solvent extraction, ion exchange, and adsorption [2,4]. Methods like electrodialysis, ion exchange and reverse osmosis have proven to be expensive and inefficient to remove copper ions to a lesser degree, while chemical treatments are rarely used because of difficulty in sludge handling and disposal apart from high maintenance cost [4].

Adsorption has become a preferred choice due to its straightforwardness, economical, and easy to scale-up. The widely used adsorbent to accomplish the process is activated carbon. It is known to possess large surface area, chemically stable and durable [5].

Commercial activated carbon, however, suffers from a number of drawbacks. Some of the precursors, like coal and petroleum pitch, are not renewable, while regeneration of the spent is relatively expensive. With the global demand for activated carbon is forecasted to be around 5–10% a year, the steep price increase is also inevitable [6]. The adsorption process thus becomes less economical because of this scenario. This has triggered a search for alternative precursor from abundantly available and inexpensive sources.

Several efforts to convert carbonaceous materials into activated carbon particularly for heavy metals remediation have been reported in the literature [7–9]. An interesting material under this category is cattle-manure-compost, a residue of temperature-phased anaerobic digestion for methane generation [10]. It can become a source of pollution and threat to public health if not properly disposed. Therefore, converting the compost into activated carbon is a good strategy to overcome the aforesaid problems and later could be used to mitigate other type of pollutions [11,12].

It is well noted that heavy metals are better adsorbed onto the carbon surface that is rich with acidic functional groups such as carboxylic and lactonic groups, to which the ion-exchange mechanism is operative [12,13]. However, such surface could not be readily developed in the activation of carbonaceous materials, in which oxidation process—that is indeed expensive—may be required [13]. To date, the extent of pores of activated carbons in the absence of acidic groups toward copper removal is yet to be explored.

This study was devoted to investigate the affinity of pores and its correlation with copper adsorption. Two assays of cattle-manure-compost-derived activated carbons were prepared prior to be tested for copper removal. Performance of each activated carbon under different pore properties was compared with the commercial Filtrasorb400 (F400). The equilibrium data were analyzed using established models, that is, Langmuir, Freundlich, and Redlich–Peterson, while the extent of adsorption was analyzed using Scatchard plots. Finally, the results and possible mechanisms governing the adsorption of copper ions were discussed.

## 2. Materials and methods

All analytical grade chemicals were purchased from Kanto Chemical Co., Inc. Commercial F400 was obtained from Calgon Mitsubishi Chemical Corporation.

### 2.1. Activated carbons

Cattle-manure-compost (C: 46.5%, H: 5.66%, N: 1.33%), a residue of temperature-phased anaerobic digestion for methane generation, was obtained from JFE Corporation, Japan. The waste was converted into activated carbons by $ZnCl_2$ at weight ratios of 0.5 and 1.5. Carbonization was progressed at 500℃ for 1 h under the flow of $N_2$ [10,12]. This was followed by heat treatment under the flow of high-purity helium at temperatures of 500, 800, and 1,000℃ for 1 h to produce activated carbons with different pore properties. Earlier studies suggested that helium gas is effective to eliminate surface functional groups at higher temperature, and such procedure could not be accomplished by using nitrogen gas alone [13–16]. The activated carbons were designated as *AxDy* where A refers to activated carbon with $x$ weight ratio, while $D$ represents heat treatment at $y$ hundred temperatures. Thus, A1.5D8 refers to activated carbon with 1.5 weight ratio and treated at 800℃.

### 2.2. Physical and chemical properties of activated carbons

Surface chemistry of activated carbons was evaluated using Boehm titration [17]. Briefly, different batches of 0.3 g of activated carbon were brought into contact with 15 mL solutions of $NaHCO_3$, $Na_2CO_3$, NaOH and HCl. Neutralization points were observed using phenolphthalein for the titration of strong base with strong acid and methyl red for titration of weak base with strong acid.

The pH of point zero charge ($pH_{PZC}$) was determined using the pH drift method [18]. It is defined as the pH at which the net surface charge equals to zero. Batches of 0.1 g carbon were brought into contact with NaCl at different initial pH and were allowed to equilibrate at 25℃ for 24 h. The value of $pH_{PZC}$ is measured when the final pH equals the initial pH.

Pore characteristics were determined using Beckman Coulter SA3100 surface area analyzer (USA) at liquid nitrogen temperature of 77 K, while the elemental composition was measured using Perkin-Elmer PE2400 microanalyzer.

### 2.3. Removal of copper ions

Stock solution of model copper-contaminated wastewater was prepared by dissolving desired weight of $CuCl_2$ $2H_2O$ in de-ionized water. Adsorption of copper ions was carried out at 25 ± 1˚C and 100 rpm for 48 h in a water bath orbital shaker. Fixed amount of activated carbon was added to the conical flasks containing 50 mL of copper solution with known concentrations. The initial solution pH was left unadjusted and was measured as 5.2 ± 0.3. The amount of metal ions adsorbed, $q_e$ (mmol/g) was calculated as $q_e = (C_0 - C_e) \times (V/m)$, where $C_0$ and $C_e$ are, respectively, the initial and equilibrium concentrations in mmol/L, $V$ (L) is the volume of solution and $m$ (g) is the mass of carbon. Concentration of copper ions was measured using atomic absorption spectroscopy (Rigaku novAA 300). All experiments were conducted thrice, and the average values were used for analysis.

## 3. Results and discussion

### 3.1. Properties of activated carbons

Results of Boehm titration and elemental analysis are shown in Table 1. In general, both A0.5 and A1.5 series showed identical trend of chemical properties with respect to temperature of heat treatment [19]. Yield of activated carbons was slightly decreased with increasing temperature. Upon the treatment, the derived activated carbons showed a slightly higher burn-off of 9% as compared to 2% for as-received F400.

Most of the carboxylic and lactonic groups of both A0.5 and A1.5 series were already liberated at 500˚C. The concentration of total acidic groups gradually decreased with increasing temperature to 1,000˚C. This was also true for F400 series. The surface of activated carbons became more basic as the treatment temperature increases. The trend was well tallied with the values of $pH_{PZC}$. In the absence of acidic groups, the basic groups are mainly attributed to electron-donating character and delocalized π-electrons on graphene layers that could behave as Lewis bases [20].

Generally, the composition of hydrogen, nitrogen, and oxygen on the surface of activated carbon decreased as the temperature increases to 800˚C. This is attributed to the release of volatiles at higher temperature. At 1,000˚C, however, the carbon content was slightly decreased with small rise in the composition of hydrogen and oxygen. It is suggested that the carbon sites became rich in electron density to which the moisture could be readily adsorbed at room temperature [14,21].

The increase in temperature also resulted in the decrease in nitrogen content of the derived activated carbons to about 65%. The leftover nitrogen moieties may consist of quaternary nitrogen, pyridinic, and pyrrolic, while the fate of nitrogen functional groups in the non-cyclized structure will be the same as that of acidic functional groups [15].

Table 2 displays the pore characteristics of activated carbons. Detail characterization of morphology and microstructure of these activated carbons has been reported elsewhere [16]. The surface area and mesopore content of A1.5 series were greater than those of A0.5 series [19]. A greater weight ratio of $ZnCl_2$ used for activation has resulted in a more intense dehydrating effect to enlarge the surface area so as to increase the mesopore content [10]. Both activated carbons derived from cattle-manure-compost

Table 1
Surface chemistry and elemental composition of activated carbons

| Activated carbons | Yield (%) | $pH_{PZC}$ | Functional groups (mmol/g) | | | | Elemental composition (daf,%) | | | |
|---|---|---|---|---|---|---|---|---|---|---|
| | | | Carboxylic | Lactonic | Phenolic | Basic | Carbon | Hydrogen | Nitrogen | Oxygen* |
| A0.5D5 | 39.2 | 7.7 | 0 | 0.02 | 0.69 | 0.47 | 85.9 | 1.37 | 2.03 | 10.7 |
| A1.5D5 | 39.7 | 8.5 | 0 | 0 | 0.78 | 0.47 | 90.4 | 1.23 | 1.82 | 6.55 |
| F400D5 | 85.6 | 9.6 | 0 | 0 | 0.42 | 0.41 | 94.2 | 0.05 | 0.44 | 5.31 |
| A0.5D8 | 36.2 | 10.2 | 0 | 0 | 0.49 | 0.59 | 92.8 | 0.09 | 1.59 | 5.52 |
| A1.5D8 | 36.6 | 10.3 | 0 | 0 | 0.52 | 0.60 | 94.6 | 0.14 | 1.38 | 3.88 |
| F400D8 | 83.9 | 10.9 | 0 | 0 | 0.44 | 0.56 | 96.0 | 0.03 | 0.62 | 3.35 |
| A0.5D10 | 35.6 | 10.4 | 0 | 0 | 0.29 | 0.74 | 91.2 | 0.45 | 0.60 | 7.75 |
| A1.5D10 | 36.4 | 10.4 | 0 | 0 | 0.28 | 0.67 | 93.5 | 0.25 | 0.70 | 5.55 |
| F400D10 | 83.9 | 10.9 | 0 | 0 | 0.27 | 0.58 | 91.2 | 0.29 | 0.34 | 8.17 |

$pH_{PZC}$: pH of point zero charge, daf: dry, ash free, *calculated by difference.

Table 2
Pore characteristics of activated carbons

| Activated carbons | Pore characteristics | | | | | | |
|---|---|---|---|---|---|---|---|
| | $A_{BET}$ (m$^2$/g) | $A_{Meso}$ (m$^2$/g) | $A_{Micro}$ (m$^2$/g) | $V_{Total}$ (ml/g) | $V_{Micro}$ (ml/g) | $R_{Meso}$ (%) | $D_{Avg}$ (nm) |
| A0.5D5 | 961 | 139 | 822 | 0.51 | 0.37 | 27 | 2.1 |
| A1.5D5 | 1,779 | 1,184 | 596 | 1.06 | 0.24 | 77 | 2.4 |
| F400D5 | 1,078 | 214 | 862 | 0.66 | 0.38 | 42 | 2.4 |
| A0.5D8 | 702 | 75 | 627 | 0.38 | 0.28 | 25 | 2.2 |
| A1.5D8 | 1,220 | 694 | 526 | 0.70 | 0.22 | 68 | 2.3 |
| F400D8 | 1,141 | 229 | 908 | 0.70 | 0.40 | 42 | 2.4 |
| A0.5D10 | 704 | 94 | 623 | 0.39 | 0.28 | 28 | 2.2 |
| A1.5D10 | 1,182 | 644 | 538 | 0.68 | 0.23 | 66 | 2.3 |
| F400D10 | 1,178 | 242 | 934 | 0.73 | 0.41 | 43 | 2.5 |

$A_{BET}$: BET surface area, $A_{Meso}$: mesopore surface area, $A_{Micro}$: micropore surface area, $V_{Total}$: total pore volume, $V_{Micro}$: micropore volume, $R_{Meso}$: mesopore content, $D_{Avg}$: average pore width.

showed a decrease in surface area with the increase in treatment temperature. Moreover, the decrease in surface area for A1.5 series was more prevalent because A1.5D5 was originally rich in mesopore structure that is prone to diminish at a higher temperature [12]. However, F400 series demonstrated almost unchanged pore properties with increasing temperature. It is obvious from Table 2 that A1.5D8 showed a decrease in mesopore content, while there is no considerable difference was noticed from its other two counterparts (A0.5D8 and F400D8). In our earlier work [12], we have reported that manure-compost-activated carbons possess less rigid structure compared with F400. Because of its mesopore-rich nature, it is suggested that the mesopores of A1.5 are further enlarged at 800°C, thus decreasing the mesopore content. Similar trend was also observed for microporous A0.5 in which the micropore content decreases at 800°C while no further changes were observed at 1,000°C, indicating that the physical properties of activated carbons produced at 800 and 1,000°C are identical. Average pore widths for activated carbons studied were within the lower edge of mesopore ranging from 2.1 to 2.5 nm.

### 3.2. Removal of copper ions

Uptake of copper ions by 500°C-treated activated carbons is illustrated in Fig. 1. Clearly, A1.5D5 displays a greater copper removal than F400D5 and A0.5D5. The highest recordable uptake of copper by A1.5D5, F400D5, and A0.5D5 were 0.10, 0.08, and 0.05 mmol/g, respectively. The possible characteristics that driven the adsorption of copper ions are surface area and mesopore content, as referred in Table 2. It is suggested that the higher the surface area the greater the interaction probabilities to accommodate copper ions. Even if the concentration of acidic groups was small, F400D5 still showed a greater uptake of copper than A0.5D5. In this instance, the roles of surface area and mesopore content outweigh the contribution of acidic functional groups toward the removal of copper [14].

Fig. 2 shows the removal of copper ions onto 800°C-treated activated carbons. F400D8 and A0.5D8 demonstrate a similar removal trend of copper ions as their 500°C counterparts. This could be due to minimum alteration of their pore properties during 800°C heat treatment. In contrast, the maximum uptake of copper by A1.5D8 reduces to 0.06 mmol/g because of decreasing surface area and mesopore content at 31 and 41%, respectively [12,19].

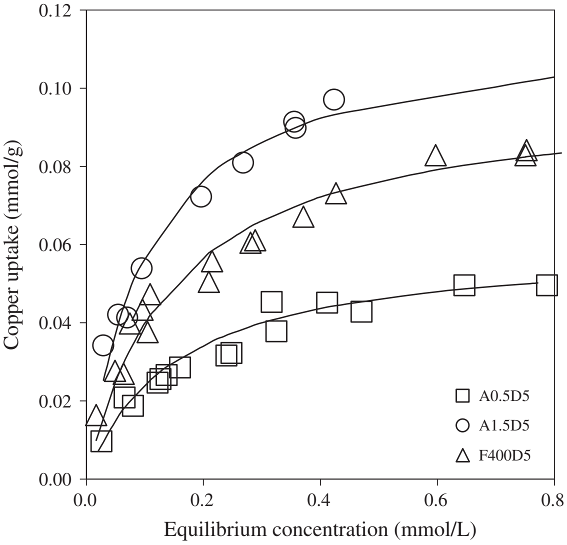

Fig. 1. Removal of copper ions by 500°C-activated carbons. Lines were predicted from Langmuir model.

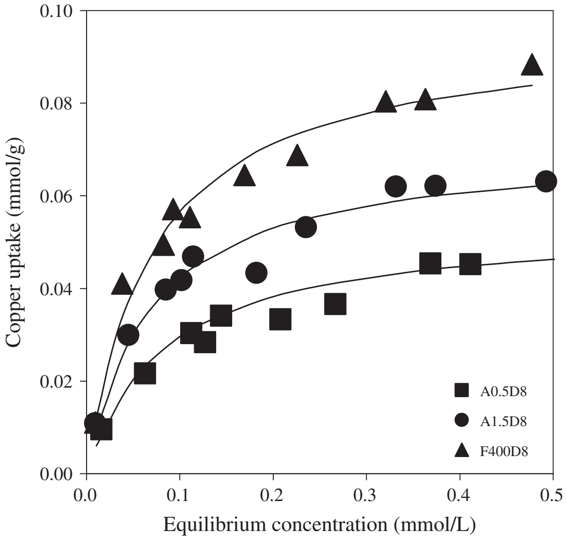

Fig. 2. Removal of copper ions by 800°C-activated carbons. Lines were predicted from Langmuir model.

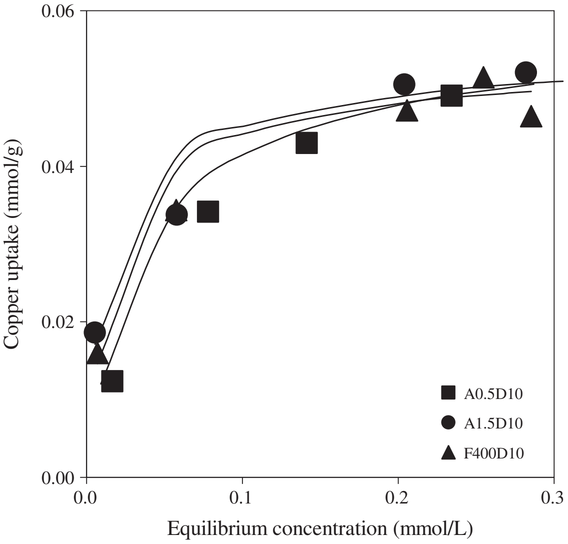

Fig. 3. Removal of copper ions by 1,000°C-activated carbons. Lines were predicted from Langmuir model.

Fig. 3 represents the removal of copper by 1,000°C treated activated carbons. As can be seen, all three activated carbons showed identical copper removal of 0.05 mmol/g despite their varying pore properties. It can be inferred from Table 2 that heat treatment from 800 to 1,000°C offers trivial effects on their pore properties. Supposedly, the 1,000°C activated carbons depicted identical trends of copper uptake as their 800°C counterparts. However, because of their electron-dense surface, copper ions are partly inhibited to enter the pores channels probably due to the competition with the protons.

### 3.3. Isotherm studies

A good adsorption process is designed upon the fundamental information and appropriate correlation of equilibrium isotherms. Three generally used isotherm models, namely Langmuir, Freundlich, and Redlich–Peterson were employed to characterize the adsorption data. The Langmuir isotherm assumes uniform monolayer adsorption on a homogeneous surface and is given by [22,23],

$$q_e = \frac{C_e \cdot Q \cdot b}{1 + b \cdot C_e} \tag{1}$$

where $Q$ and $b$ represent maximum uptake and affinity, respectively. The Freundlich isotherm describes multilayer adsorption on a heterogeneous surface and is given by [24],

$$q_e = K_F \cdot C_e^{\frac{1}{n}} \tag{2}$$

where $K_F$ and $n$ are Freundlich constants related to the uptake capacity and intensity, respectively. The Redlich–Peterson isotherm combines the features of the Langmuir and Freundlich models and can be described as follows [25],

$$q_e = \frac{A \cdot C_e}{1 + B \cdot C_e^g} \tag{3}$$

$A$, $B$, and $g$ are all the Redlich–Peterson constants, where $0 < g < 1$. When $g$ equals to unity, the Redlich–Peterson isotherm becomes Langmuir isotherm, while it transforms to Henry's law when $g$ is zero. The three non-linear models were solved using *Solver* add-in for optimum correlation of determination ($r^2$).

Equilibrium values of solution pH, parameters of isotherm models and coefficients of determination ($r^2$) are tabulated in Table 3. The adsorption of copper ions can be well described by the three isotherm models, but it was found that the Langmuir model was more fitted to linear approximation than the other two models. This was true for all activated carbons studied. The $1/n$ values of Freundlich isotherm which vary between 0.2 and 0.4 imply the homogeneous surface nature of activated carbons, while reasonable $g$ values of Redlich–Peterson isotherm that close to unity also indicated the normal feature of Langmuir isotherm. As can be seen in Figs. 1–3, the predicted lines from Langmuir model were well agreed to the experimental data.

The increase in equilibrium pH in adsorption suggested that the surface of activated carbons was protonated and becomes positively charged. The consistent values of equilibrium pH suggested that

Table 3
Equilibrium pH and isotherm constants for copper removal by activated carbons

| Activated carbons | $pH_e$ | Langmuir isotherm | | | Freundlich isotherm | | | Redlich–Peterson isotherm | | | |
|---|---|---|---|---|---|---|---|---|---|---|---|
| | | $Q$ (mmol/g) | $b$ (L/mmol) | $r^2$ | $K_F$ | $1/n$ | $r^2$ | $A$ (L/g) | $B$ | $g$ | $r^2$ |
| A0.5D5 | 5.5 ± 0.2 | 0.060 | 6.70 | 0.96 | 0.057 | 0.36 | 0.94 | 0.591 | 9.93 | 0.85 | 0.96 |
| A0.5D8 | 6.0 ± 0.1 | 0.054 | 12.1 | 0.97 | 0.064 | 0.36 | 0.97 | 2.06 | 33.7 | 0.74 | 0.97 |
| A0.5D10 | 6.3 ± 0.1 | 0.056 | 28.0 | 0.99 | 0.081 | 0.33 | 0.94 | 1.72 | 29.4 | 0.97 | 0.98 |
| A1.5D5 | 5.4 ± 0.2 | 0.117 | 9.46 | 0.98 | 0.139 | 0.41 | 0.98 | 3.15 | 22.9 | 0.68 | 0.98 |
| A1.5D8 | 6.3 ± 0.2 | 0.071 | 14.7 | 0.98 | 0.086 | 0.34 | 0.94 | 1.84 | 23.5 | 0.83 | 0.97 |
| A1.5D10 | 6.4 ± 0.1 | 0.052 | 65.7 | 0.93 | 0.064 | 0.21 | 0.91 | 8.22 | 138 | 0.87 | 0.88 |
| F400D5 | 5.8 ± 0.1 | 0.099 | 6.78 | 0.98 | 0.096 | 0.37 | 0.97 | 1.65 | 16.8 | 0.74 | 0.97 |
| F400D8 | 6.3 ± 0.2 | 0.096 | 14.2 | 0.97 | 0.118 | 0.35 | 0.96 | 2.40 | 22.3 | 0.82 | 0.97 |
| F400D10 | 6.4 ± 0.1 | 0.052 | 48.6 | 0.96 | 0.072 | 0.28 | 0.96 | 5.12 | 81.7 | 0.84 | 0.92 |

$pH_e$: equilibrium pH.

the amount of protons adsorbed for each activated carbon is uniform regardless the increase of copper concentration in adsorption. Therefore, it is adequate to utilize single-component isotherm models to represent the adsorption data.

In general, the increase in equilibrium pH occurs when the surface of activated carbon is absent from acidic functional groups and becomes lesser than $pH_{PZC}$. This commonly results in a lower uptake of copper ions due to repulsive force from the surface. Attempt to increase the solution pH above $pH_{PZC}$ in order to promote negatively charged surface so as to enhance the uptake of copper ions will only give better chance for precipitate complex to evolve and thereafter nullify the adsorptive removal.

When acidic functional groups that behave as electron withdrawers are liberated in helium treatment at higher temperature, the π-system becomes rich in electron density and thus operative for metal ions adsorption through Cπ–cation interaction [13,15]. This could also be the reason for the increase in affinity toward copper ions, regardless the decrease in surface area as noticeably reported for A1.5 series in Tables 2 and 3. It is worth to note that the active sites for adsorption are directly dependant on surface area and pore volume. Therefore, it could be adequately inferred that the electron density in A1.5D5 was deficient in comparison with that of A1.5D8 and A1.5D10.

A1.5 series showed a greater affinity than the other two activated carbons series.

This could be explained by its mesopore-rich nature. Affinity is commonly referred to a higher removal at lower equilibrium concentration. From Figs. 1–3, for instance, A0.5D10 (affinity: 28 L/mmol) showed a superior removal performance as compared to A0.5D8 (affinity: 12 L/mmol) and A0.5D5 (7 L/mmol) at equilibrium concentration below 0.3 mmol/L.

The fact that copper ions have to compete with protons to occupy active sites rich in electron density is undeniable. F400D5 showed a higher equilibrium pH, thus a greater amount of protons adsorbed (0.008 mmol/g) than A0.5D5 and A1.5D5 (0.005 mmol/g), because of its less acidic in nature. At 1,000 °C, the increase in surface affinity for copper ions also attracts 0.010 mmol/g protons to be adsorbed as well. This can be verified from the equilibrium pH that increases with increasing treatment temperature of activated carbon. In aqueous solution, the values of hydrated (effective) ionic radii for copper ions and protons are 4.2 and 9.0 Å, respectively [26]. It is notable that the bigger the ionic radii the lesser the usage of energy for dehydration, thus the greater its propensity to occupy the adsorbent sites. This sufficiently explains the lower copper uptake onto A1.5D10 and F400D10 due to most of their surface sites have been resided by protons.

Also, it is presumed that protons are only adsorbed onto the mesopore channels (2–50 nm), and left the micropore channels (<2 nm) unoccupied. This is supported by a similar uptake of copper by 1,000 °C activated carbons that conformed to their comparable values of micropore surface area. Furthermore, a greater removal onto F400D8 ($A_{Micro}$: 908 $m^2/g$) above A1.5D8 ($A_{Micro}$: 526 $m^2/g$) also suggests that copper ions only utilize micropore channels for adsorption after the mesopore channels were lodged by protons.

### 3.4. Scatchard plot analysis

The analysis using Scatchard plot is employed to investigate the stability constant that bind the metal ions onto the surface of activated carbons [27,28]. Scatchard equation is given as

$$\frac{n}{[Cu]} = K(n_i - n) \tag{4}$$

where $n$ (mmol/g) is moles of copper adsorbed onto activated carbon, $[Cu]$ (mmol/L) is equilibrium concentration of copper in solution, $K$ (L/mmol) is stability constant and $n_i$ (mmol/L) is moles of maximum copper adsorbed by all sites. The values of $K$ and $n_i$ are obtained from the slope and intercept of the plot $n/[Cu]$ against $n$.

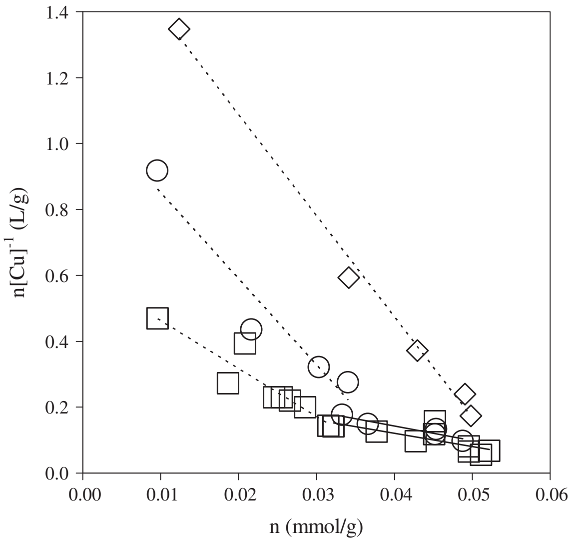

Fig. 4. Scatchard plots for the binding of copper onto A0.5 series activated carbons: (□) A0.5D5, (○) A0.5D8, (*Δ*) A0.5D10.

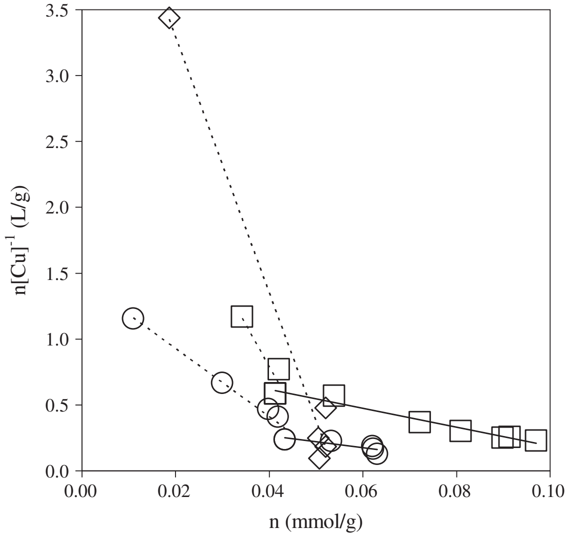

Fig 5. Scatchard plots for the binding of copper onto A1.5 series activated carbons: (□) A1.5D5, (○) A1.5D8, (*Δ*) A1.5D10.

Figs. 4–6 show the Scatchard plots for A0.5, A1.5, and F400-activated carbons series, respectively. It is interesting to observe the two inter-connected straight lines for all 500- and 800℃-activated carbons studied. It explicitly indicates that two stability constants for different active sites exist to cooperatively bind the copper ions [29,30].

The stability constant and maximum uptake yielded from the Scatchard plots are given in Table 4. In general, the first stability constant, $K_1$ (dashed line) corresponds to copper uptake onto one active site at lower equilibrium concentrations, while $K_2$ (solid line) relates to another active site when the surface approaching saturation at higher equilibrium concentrations. It is suggested that the site $K_1$ may be belonged to the mesopores exhibited a higher affinity

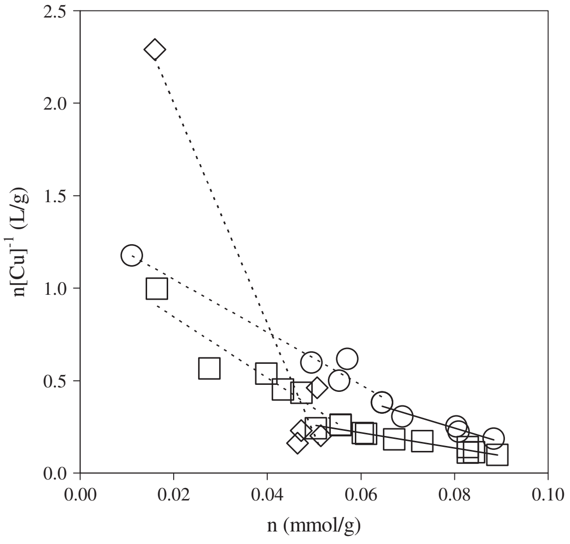

Fig. 6. Scatchard plots for the binding of copper onto F400 series activated carbons: (□) F400D5, (○) F400D8, (*Δ*) F400D10.

Table 4
Constants of Scatchard plots

| Activated carbons | $K_1$ (L/mmol) | $n_1$ (mmol/g) | $K_2$ (L/mmol) | $n_2$ (mmol/g) |
|---|---|---|---|---|
| A0.5D5 | 14.5 | 0.042 | 4.06 | 0.070 |
| A0.5D8 | 26.1 | 0.043 | 4.40 | 0.072 |
| A0.5D10 | 30.7 | 0.055 | – | – |
| A1.5D5 | 63.6 | 0.052 | 7.17 | 0.126 |
| A1.5D8 | 25.8 | 0.056 | 4.53 | 0.099 |
| A1.5D10 | 97.0 | 0.054 | – | – |
| F400D5 | 16.5 | 0.071 | 4.13 | 0.113 |
| F400D8 | 14.3 | 0.093 | 7.65 | 0.112 |
| F400D10 | 59.7 | 0.054 | – | – |

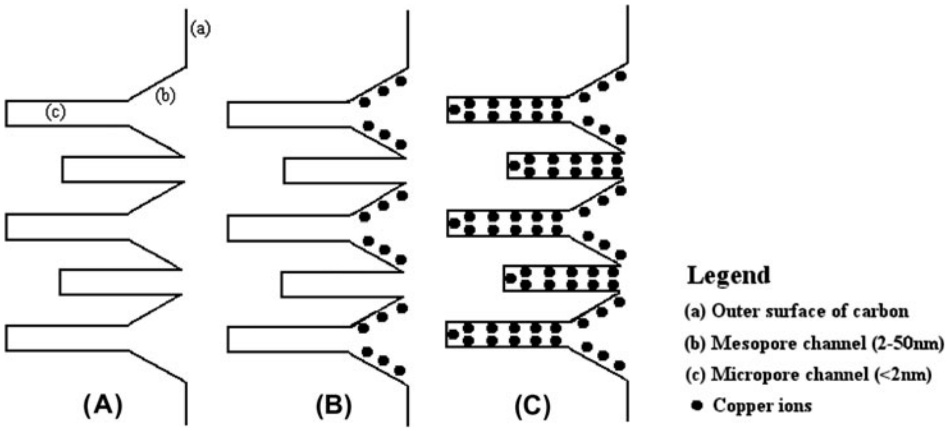

Fig. 7. Schematic representation of copper uptake by heat treated-activated carbons: (A) surface of no contact with copper ions, (B) surface at low equilibrium concentrations of copper ions, and (C) surface at higher equilibrium concentrations so as approaching surface saturation.

toward copper ions and protons than the micropores (site $K_2$). This summarizes that copper ions preferably adsorb onto the mesopores at lower equilibrium concentrations and switched to the micropores at higher equilibrium concentrations.

For all 1,000˚C-activated carbons, only one-connected straight line that represents Scatchard constants was detected (dashed lines). Similar to a previous explanation, the $K_1$ constants refer to copper binding affinity onto mesopore channels. These constants are comparable with the values presented under Langmuir constants in Table 3. Similar to that of adsorption affinity, the stability constant also increased with increasing treatment temperature.

The mechanisms of copper ions removal on the pores of activated carbon can be visualized in Fig. 7. It is believed that the adsorption of copper ions is driven by the higher affinity sites of mesopore (b) at lower equilibrium concentrations, and thereafter switches to the lower affinity sites of micropore (c) at higher equilibrium concentrations.

In the absence of acidic functional groups and under the electron-dense surface, dots in Fig. 4(B) could also be substituted into protons, while copper ions only lodge onto the micropore channels.

Therefore, in the absence or acidic functional groups, a mesoporous-activated carbon is better suited for high-affinity copper removal. It was proven that A1.5 shows a superior copper removal than F400 even without the need of further heat treatment. Due to its rich mesopore content, cattle-manure-compost-derived activated carbon is foreseen as a promising and economical candidate for high affinity copper adsorption.

## 4. Conclusions

Two assays of cattle-manure-compost-based activated carbons and a commercial F400 were treated under helium at different temperatures to promote different pore characteristics. The surface area of activated carbons decreased and became more basic as the temperature increases. The adsorption data were suited to Langmuir model which describes monolayer adsorption onto homogenous surface. Surface affinity toward adsorption was found increased with increasing temperature due to the increase in electron density on graphene layers, regardless the decrease in surface area. At lower equilibrium concentrations, copper ions preferably adsorbed onto the mesopores and shifted to the micropores as the surface reaching saturation. The extent of adsorption by Scatchard plots suggested that the mesopores and micropores cooperatively bind the copper ions, where the affinity of the former was considerably higher than that of the latter. The mesopore-rich activated carbon could offer a high-affinity removal of copper without the need of further oxidation and heat treatment.

## Acknowledgments

The corresponding author (M.A.A. Zaini) wishes to dedicate this work to Prof. Dr. Hideki Tatsumoto. He also thanked Ministry of Higher Education Malaysia and Universiti Teknologi Malaysia (UTM) for the *SLAI*-financial aid. This work was funded in part by Japan Society for the Promotion of Science under Grants-in-aid for Scientific Research (C) (No. 23510091). Support from the UTM-Research University Grants, 77974 and 03J20, is gratefully acknowledged.

## References

[1] National Research Council, Copper in Drinking Water, National Academy Press, Washington, 2000.

[2] N.K. Lazaridis, E.N. Peleka, Th.D. Karapantsios, K.A. Matis, Copper removal from effluents by various separation techniques, Hydrometallurgy 74 (2004) 149–156.

[3] WHO, Guidelines for Drinking Water Quality, World Health Organization, Geneva, 2006.

[4] T.A. Kurniawan, G.Y.S. Chan, W.-H. Lo, S. Babel, Physico-chemical treatment techniques for wastewater laden with heavy metals, Chem. Eng. J. 118 (2006) 83–98.

[5] R.C. Bansal, M. Goyal, Activated Carbon Adsorption, Taylor & Francis, New York, NY, 2005.

[6] Roskill. The Economics of Activated Carbon, Roskill Information Services Ltd., London, 2008.

[7] Muhammad, T.G. Chuah, Y. Robiah, A.R. Suraya, T.S.Y. Choong, Single and binary adsorptions isotherms of Cd(II) and Zn(II) on palm kernel shell based activated carbon, Desalin. Water Treat. 29 (2011) 140–148.

[8] K. Li, Y. Li, H. Hu, Adsorption characteristics of lead on cotton-stalk-derived activated carbon fibre by steam activation, Desalin. Water Treat. 30 (2011) 1–9.

[9] J.M. Dias, M.C.M. Alvim-Ferraz, M.F. Almeida, J. Rivera-Utrilla, M. Sánchez-Polo, Waste materials for activated carbon preparation and its use in aqueous-phase treatment: a review, J. Environ. Manage. 85 (2007) 833–846.

[10] Q. Qian, M. Machida, H. Tatsumoto, Preparation of activated carbons from cattle-manure compost by zinc chloride activation, Bioresour. Technol. 98 (2007) 353–360.

[11] Q. Qian, Q. Chen, M. Machida, H. Tatsumoto, K. Mochidzuki, A. Sakoda, Removal of organic contaminants from aqueous solution by cattle manure compost (CMC) derived activated carbons, Appl. Surf. Sci. 255 (2009) 6107–6114.

[12] M.A.A. Zaini, R. Okayama, M. Machida, Adsorption of aqueous metal ions on cattle-manure-compost based activated carbons, J. Hazard Mater. 170 (2009) 1119–1124.

[13] S. Sato, K. Yoshihara, K. Moriyama, M. Machida, H. Tatsumoto, Influence of activated carbon surface acidity on adsorption of heavy metal ions and aromatics from aqueous solution, Appl. Surf. Sci. 253 (2007) 8554–8559.

[14] J.A. Menendez, J. Phillips, B. Xia, L.R. Radovic, On the modification and characterization of chemical surface properties of activated carbon: in the search of carbons with stable basic properties, Langmuir 12 (1996) 4404–4410.

[15] M. Machida, T. Mochimaru, H. Tatsumoto, Lead(II) adsorption onto the graphene layer of carbonaceous materials in aqueous solution, Carbon 44 (2006) 2681–2688.

[16] Q. Qian, M. Machida, H. Tatsumoto, Textural and surface chemical characteristics of activated carbons prepared from cattle manure compost, Waste Manage. 28 (2008) 1064–1071.

[17] H.P. Boehm, Some aspects of the surface chemistry of carbon blacks and other carbons, Carbon 32 (1994) 759–769.

[18] I.D. Smiciklas, S.K. Milonjic, P. Pfendt, S. Raicevic, The point of zero charge and sorption of cadmium (II) and strontium (II) ions on synthetic hydroxyapatite, Sep. Purif. Technol. 18 (2000) 185–194.

[19] M.A.A. Zaini, M.A. Che-Yunus, Y. Amano, M. Machida, Relationship between helium degassing of cattle-manure-compost adsorbents and copper ions removal, Int. J. Org. Chem. 2 (2012) 262–266.

[20] M.A. Montes-Moran, D. Suarez, J.A. Menendez, E. Fuente, On the nature of basic sites on carbon surface. An overview, Carbon 42 (2004) 1219–1224.

[21] Q. Qian, S. Sunohara, Y. Kato, M.A.A. Zaini, M. Machida, H. Tatsumoto, Water vapor adsorption onto activated carbons prepared from cattle manure compost (CMC), Appl. Surf. Sci. 254 (2008) 4868–4874.

[22] I. Langmuir, The constitution and fundamental properties of solids and liquids. Part I. Solid, J. Am. Chem. Soc. 38 (1916) 2221–2295.

[23] I. Langmuir, The adsorption of gases on plane surfaces of glass, mica and platinum, J. Am. Chem. Soc. 40 (1918) 1361–1403.

[24] H.M.F. Freundlich, Über die adsorption in lösungen, Z. Phys. Chem. 57A (1906) 385–470.

[25] O. Redlich, D.L. Peterson, A useful adsorption isotherm, J. Phys. Chem. 63 (1959) 1024.

[26] D.R. Lide, CRC Handbook of Chemistry and Physics, 82nd ed., CRC Press, Boca Raton, 2001.

[27] Y.I. Henis, A. Levitzki, An analysis on the slope of Scatchard plots, Eur. J. Biochem. 71 (1976) 529–532.

[28] M.M. Saeed, M. Ahmed, Retention, kinetics and thermodynamics profile of cadmium adsorption from iodide medium onto polyurethane foam and its separation from zinc bulk, Anal. Chim. Acta 525 (2004) 289–297.

[29] Z. Gu, X. Wang, X. Gu, J. Cheng, L. Wang, L. Dai, M. Cao, Determination of stability constants for rare earth elements and fulvic acids extracted from different soils, Talanta 53 (2001) 1163–1170.

[30] A.A. Saboury, N. Sarri-Sarraf, S. Saidian, Thermodynamics of binding copper ion by myelin basic protein, Thermochim. Acta 381 (2002) 147–151.